



# XIII International conference on Calorimetry in High Energy Physics



## ***Measurement and simulation of the neutron detection efficiency with a Pb-SciFi calorimeter***

***M. Martini***

*Laboratori Nazionali di Frascati & Dip. Energetica Univ. Roma La Sapienza*

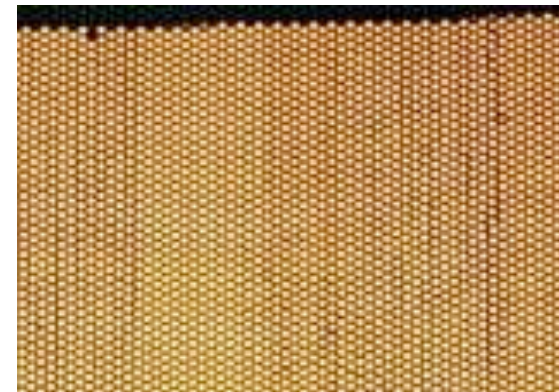
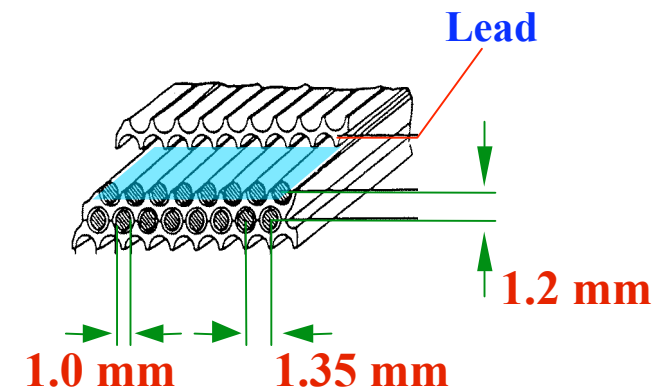
*for the KLONE Group*

M.Anelli, G.Battistoni, S.Bertolucci, C.Bini, P.Branchini, C.Curceanu,  
G.De Zorzi, A.Di Domenico, B.Di Micco, A.Ferrari, S.Fiore, P.Gauzzi,  
S.Giovannella, F.Happacher, M.Iliescu, M.Martini, S.Miscetti,  
F.Nguyen, A.Passeri, A.Prokofiev, P.Sala, B.Sciascia, F.Sirghi

# The KLOE calorimeter

Pb - scintillating fiber sampling calorimeter  
of the KLOE experiment at DAΦNE  
(LNF):

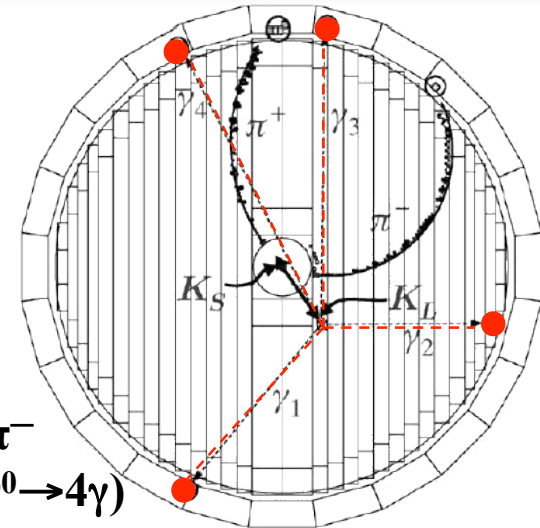
- 1 mm diameter sci.-fi. (Kuraray SCSF-81 and Pol.Hi.Tech 0046)
  - Core: polystyrene,  $\rho = 1.050 \text{ g/cm}^3$ ,  $n=1.6$ ,  
 $\lambda_{\text{peak}} \sim 460 \text{ nm}$
- 0.5 mm grooved lead foils
- Lead:Fiber:Glue volume ratio = 42:48:10
- $X_0 = 1.6 \text{ cm}$   $\rho=5.3 \text{ g/cm}^3$
- Calorimeter thickness = 23 cm
- Total scintillator thickness  $\sim 10 \text{ cm}$



# The KLOE calorimeter

Operated from 1999 to 2006

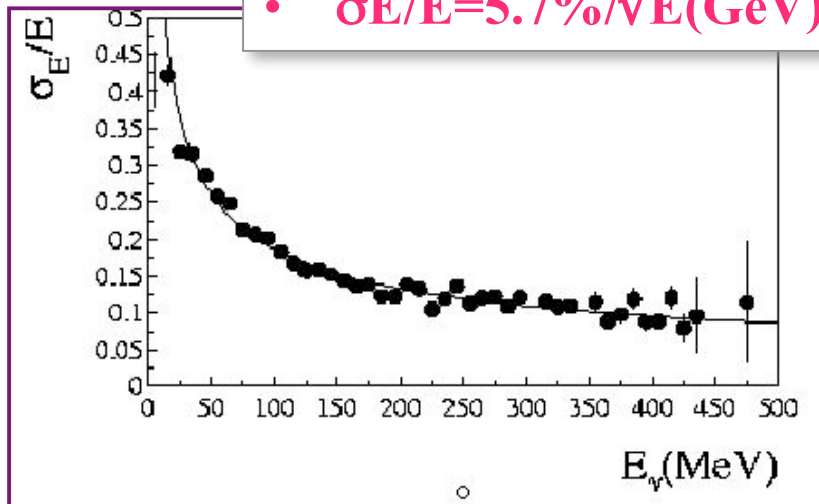
- good performance and high efficiency for electron and photon detection
- good capability of  $\pi/\mu/e$  separation



$(\phi \rightarrow K_S K_L; K_S \rightarrow \pi^+ \pi^-$   
 $K_L \rightarrow 2\pi^0 \rightarrow 4\gamma)$

Energy resolution:

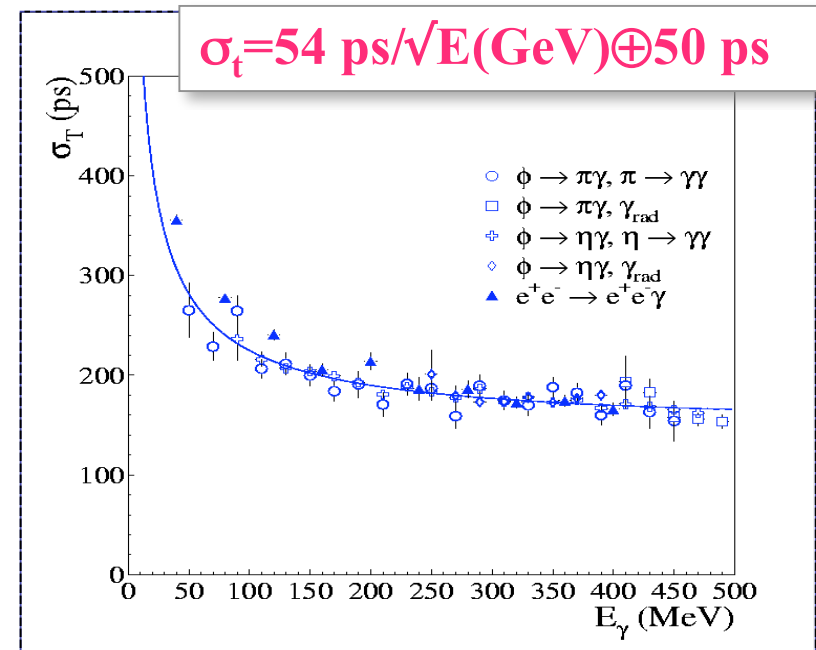
- $\sigma E/E = 5.7\%/\sqrt{E(\text{GeV})}$



(see KLOE Collaboration, NIM A482 (2002),364)

Time resolution:

- $\sigma_t = 54 \text{ ps}/\sqrt{E(\text{GeV})} \oplus 50 \text{ ps}$



# *Why neutrons at KLOE ?*

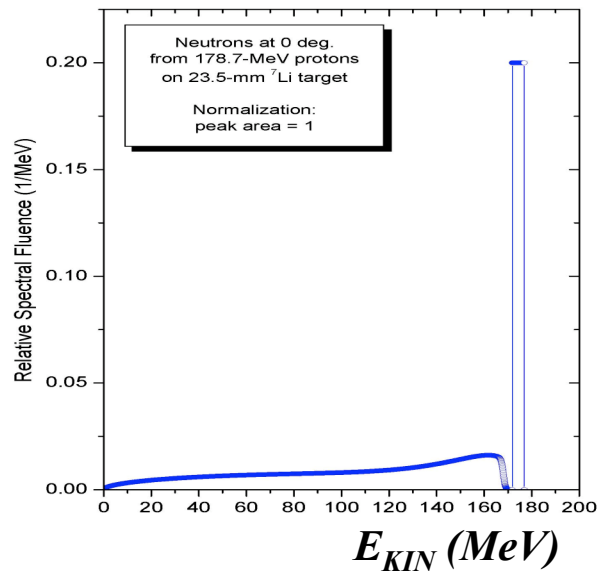
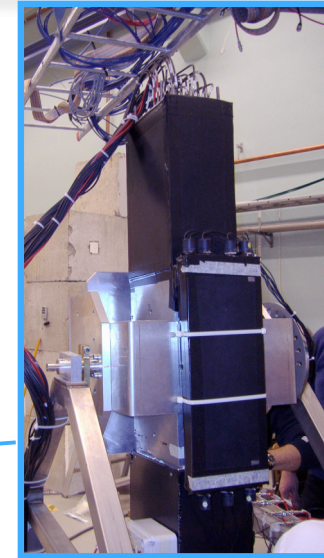
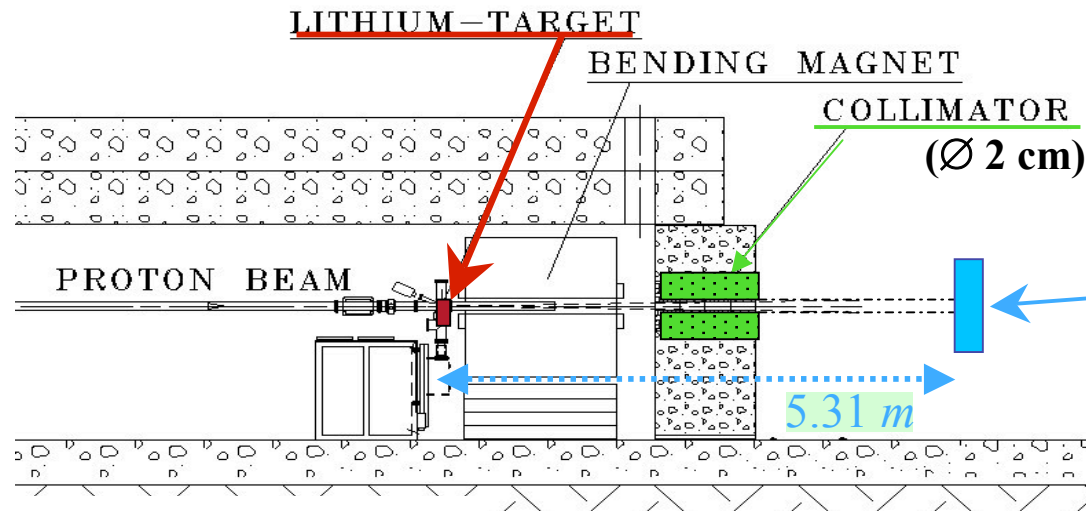
- Detection of  $n$  of few to few hundreds MeV is traditionally performed with organic scintillators (elastic scattering of  $n$  on H atoms produces protons detected by the scintillator itself)
  - ⇒ efficiency scales with thickness ⇒ **1%/cm**
- Use of high-Z material improves neutron efficiency  
(see C.Birattari et al., NIM A297 (1990) and NIM A338 (1994)  
and also T.Baumann et al., NIM B192 (2002))
- Preliminary estimate with KLOE data ( $n$  produced by  $K^-$  interactions in the apparatus) showed a high efficiency ( $\sim 40\%$ ) for neutrons with  $E_n < 20$  MeV, confirmed by the KLOE Monte Carlo
- $n$  detection is relevant for the DAΦNE-2 program at LNF; two proposals:
  - search for deeply bounded kaonic nuclei (AMADEUS)
  - measurement of the neutron time-like form factors (DANTE)

**Test been performed with neutron beam at the “The Svedberg Laboratory” (TSL) of Uppsala (October 2006 and June 2007)**



# Measurement @ TSL

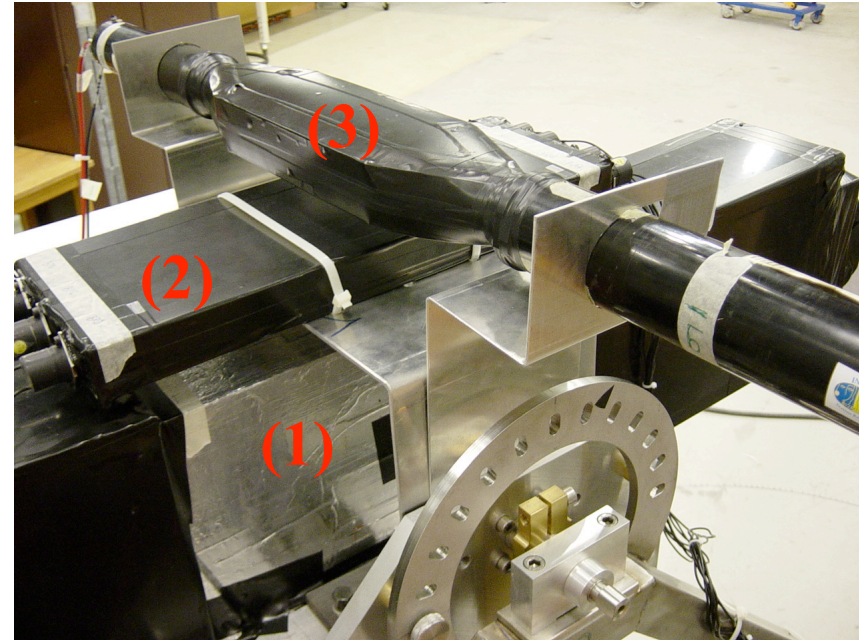
## Neutron beam



- A quasi-monoenergetic neutron beam is produced in the reaction  ${}^7\text{Li}(p,n){}^7\text{Be}$ .
- Proton beam energy from **180 MeV** to **~ 20 MeV**
- Neutron energy spectrum peaked at max energy (at 180 MeV  $f_p = 42\%$  of neutrons in the peak)
- Tail down to thermal neutrons

# Experimental setup

1. Old KLOE prototype:
  - total length **~60 cm**
  - **3×5 cells** (4.2 cm × 4.2 cm)
  - read out at both ends by Hamamatsu/Burle PMTs
2. Beam Position Monitor:  
array of 7 scintillating counters  
1 cm thickness (single side PM)
3. Reference counter :  
NE110; 5 cm thick; 10×20 cm<sup>2</sup> area  
(in June 2007 ⇒ two other NE110 counters 2.5 cm thick)



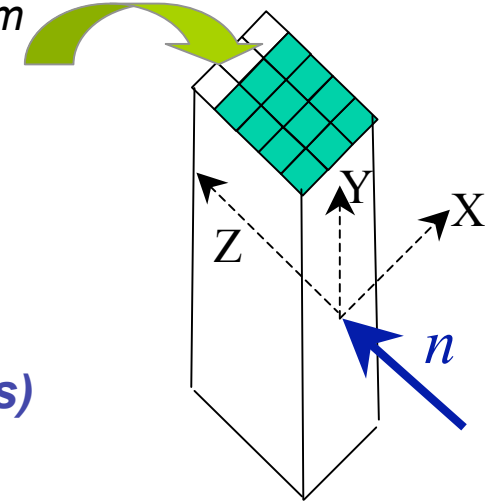
All mounted on a rotating frame allowing for vertical (data taking with  $n$  beam) and horizontal (for calibration with cosmic rays) positions

# Trigger & DAQ

## Trigger

- No beam extraction signal available
- **Scintillator trigger:** Side 1 – Side 2 overlap coincidence
- **Calorimeter trigger:** analog sum of the signals of the first 12 cells (4 planes out of 5)  
⇒  $\Sigma_A \cdot \Sigma_B$  overlap coincidence
- Trigger signal phase locked with the RF signal (45 - 54 ns)

last plane not integrated in the acquisition system



## DAQ

- Simplified version of the KLOE experiment DAQ system (VME standard)
- Max DAQ rate : 1.7 kHz - Typical run:  $10^6$  events
- For each configuration/energy: scans with different trigger thresholds
- Three data-sets:
  - $E_{peak} = 180 \text{ MeV}$  -- October 2006 - two weeks
  - $E_{peak} = 46.5 \text{ MeV}$  -- June 2007
  - $E_{peak} = 21.8 \text{ MeV}$  -- “ } 4 days

# Method of measurement

## Global efficiency measurement

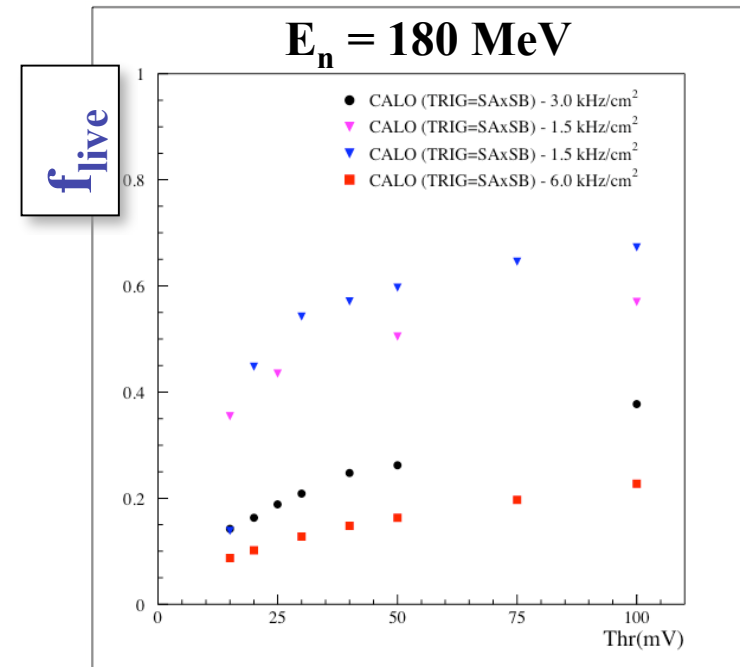
integrated on the full energy spectrum

$$\varepsilon = \frac{R_{\text{TRIGGER}}}{R_{\text{NEUTRON}} \times f_{\text{LIVE}} \times \alpha}$$

$R_{\text{NEUTRON}}$ : from beam monitor via neutron flux intensity measured by TSL.

$f_{\text{LIVE}}$ : fraction of DAQ live time

$\alpha$ : acceptance  
assuming the beam fully contained in the calorimeter surface:  
 $\alpha \approx 1$



$R_{\text{TRIGGER}}$  must be corrected for a sizeable beam halo



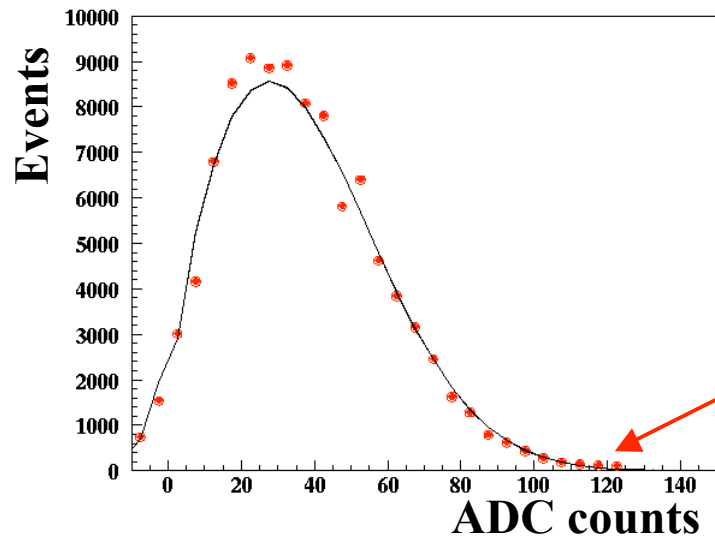
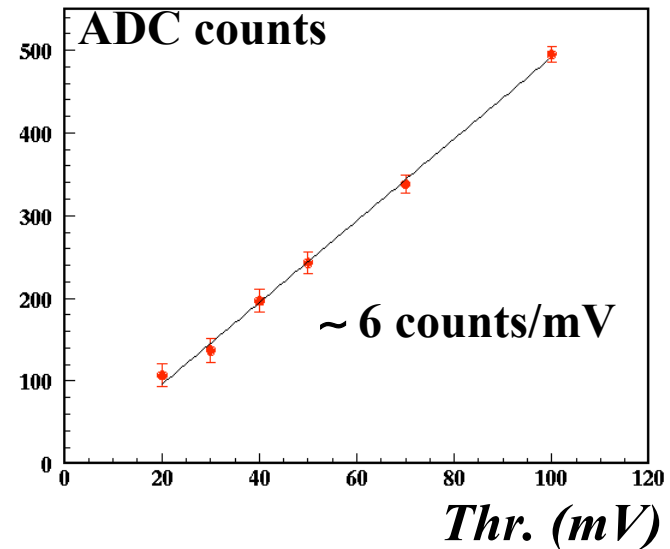
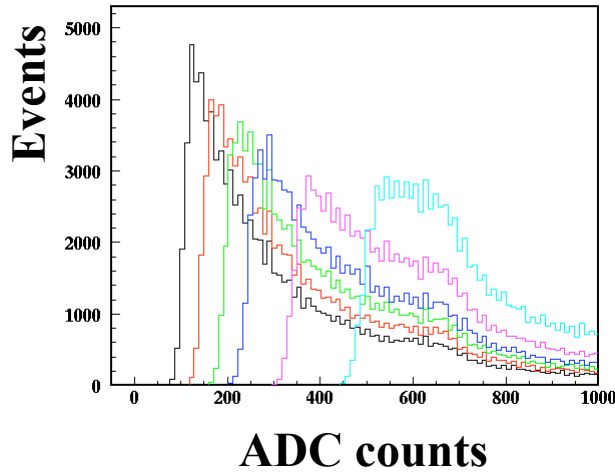
# Neutron rate

- **Absolute flux of neutrons measured after the collimator**  
**2 monitors of beam intensity (see A.Prokofiev et al., PoS (FNDA2006) 016):**
  - **Ionization Chamber Monitor (7 cm  $\varnothing$ ):**  
online monitor, not position sensitive
  - **Thin-Film Breakdown Counter (1 cm  $\varnothing$ ):**  
offline monitor; used to calibrate the ICM  
by measuring the neutron flux  
at the collimator exit
- **$\text{Rate}(n) = \text{Rate}(\text{ICM}) \cdot K \cdot \pi r^2 / f_p$**   
 $r =$  collimator radius (1 cm)  
 $K =$  calibration factor (TFBC to ICM)  
 $f_p =$  fraction of neutrons in the peak  
  
 $\Rightarrow$  accuracy: 10% at higher peak energy (180 MeV)  
20% at lower peak energy (20 – 50 MeV)



# Scintillator calibration

- *Trigger threshold calibration in MeV eq.el.en.:*



*β source to set the energy scale in MeV:*

*<sup>90</sup>Sr β<sup>-</sup> endpoint = 0.56 MeV*

*<sup>90</sup>Y β<sup>-</sup> endpoint = 2.28 MeV*

*25 keV/ADC count*

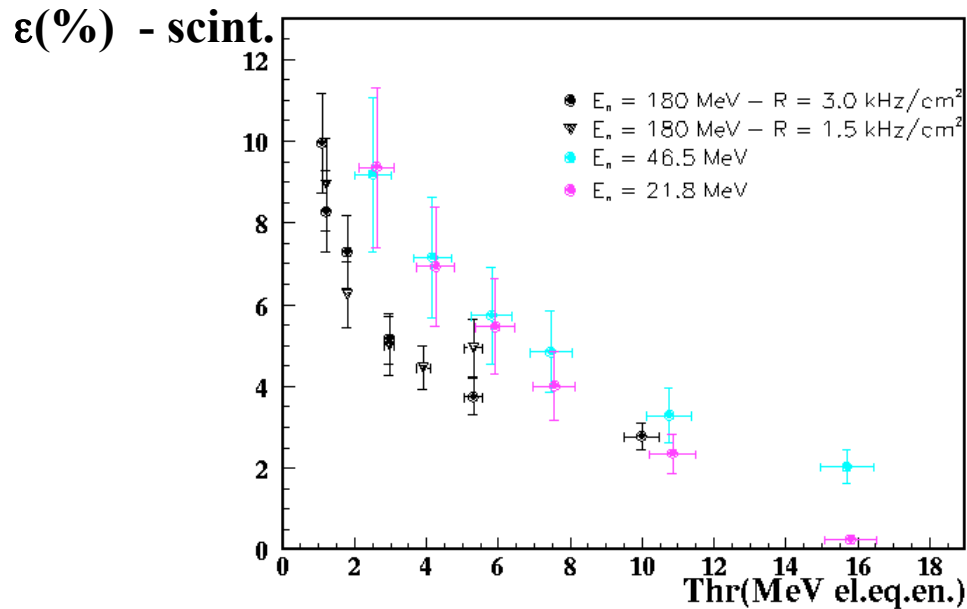


Thr. [mV]	20 → 100
Thr. [MeV]	2.5 → 15

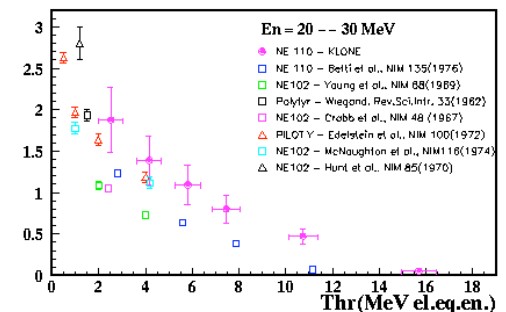
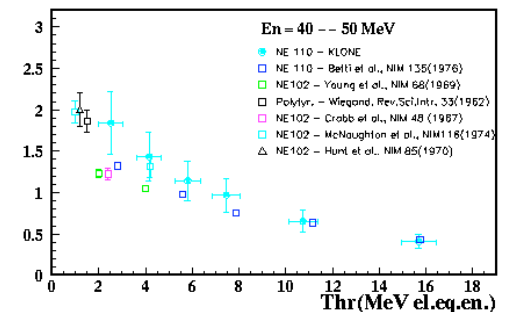
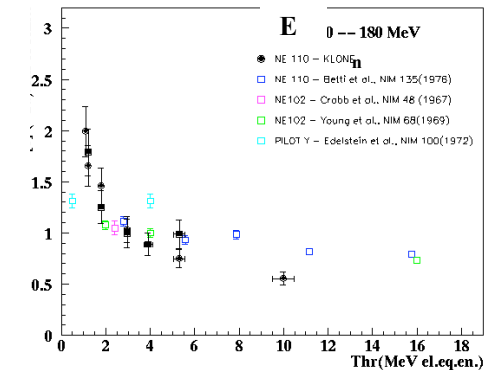


# Scintillator efficiency

- Agrees with the “thumb rule” (1%/cm) at thresholds above 2.5 MeV el.eq.en.



$\epsilon(\%)/$  cm of scintillator



- Agrees with previous measurements in the same energy range after rescaling for the thickness

Larger errors at low energies due to:

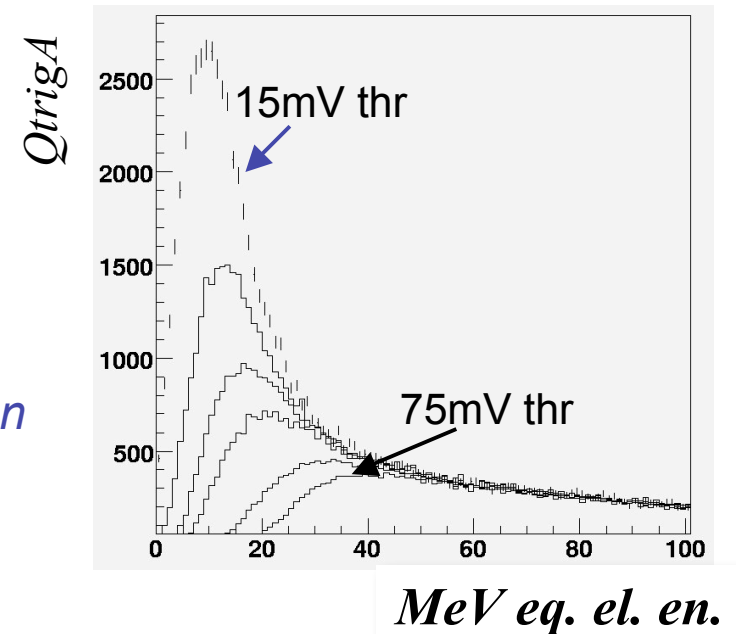
- big uncertainty in the beam halo evaluation
- worse accuracy of the beam monitors

Correction factor for beam halo  $\approx 0.9 \pm 0.1$

# Calorimeter calibration

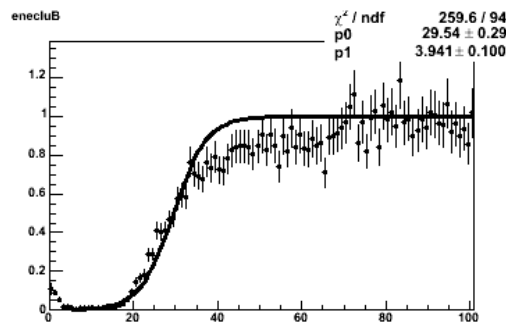
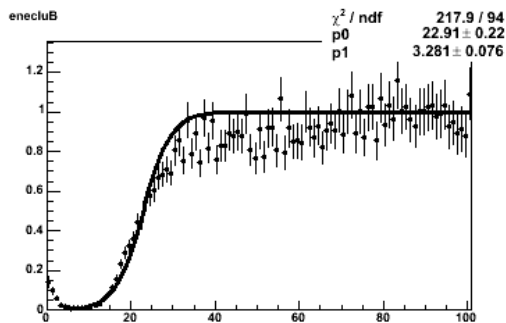
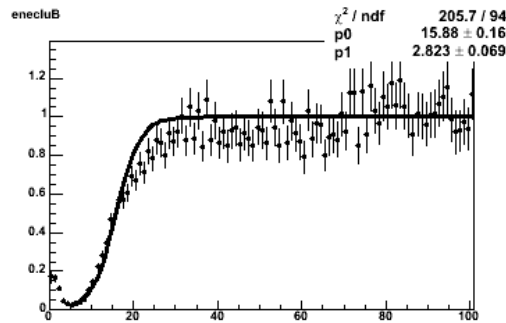
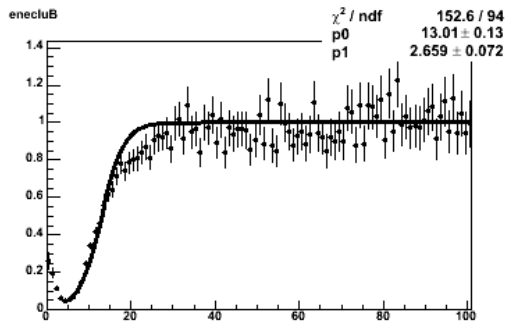
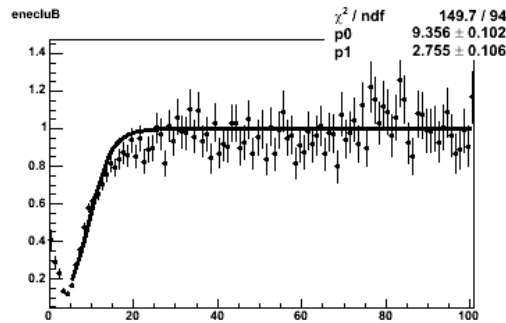
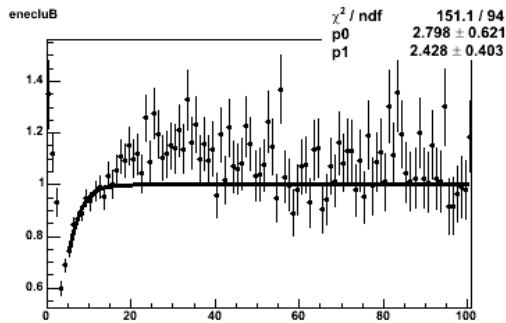
## Trigger threshold calibration

- From data sets taken at different thresholds, the distributions of the discriminated signals of  $\Sigma_A$ ,  $\Sigma_B$  have been fit with a Fermi-Dirac function to evaluate:
  - **cutoff in trigger energy**
  - **width of the used energy in MeV**
- Same exercise with the sum of the cluster energies side A and B

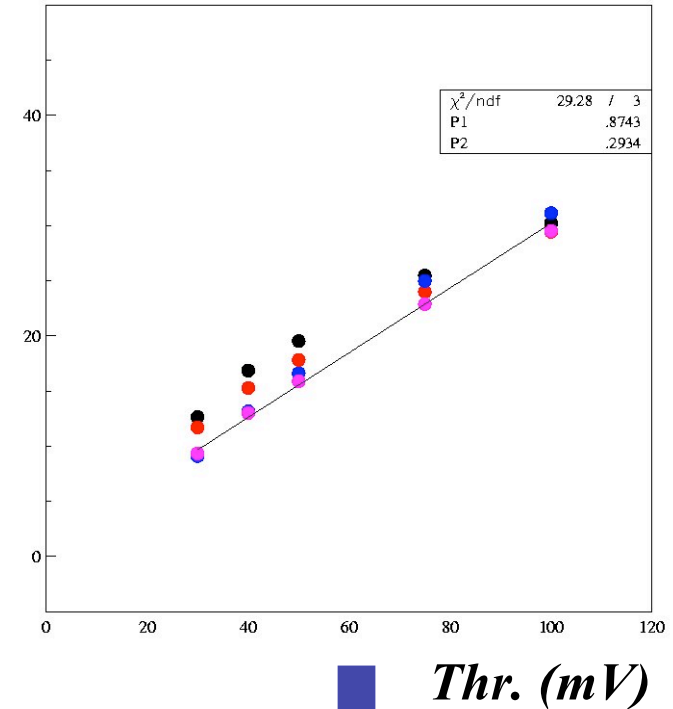


# Calorimeter calibration

(ex.) Fermi-Dirac fits for the sum of the cluster energy side B



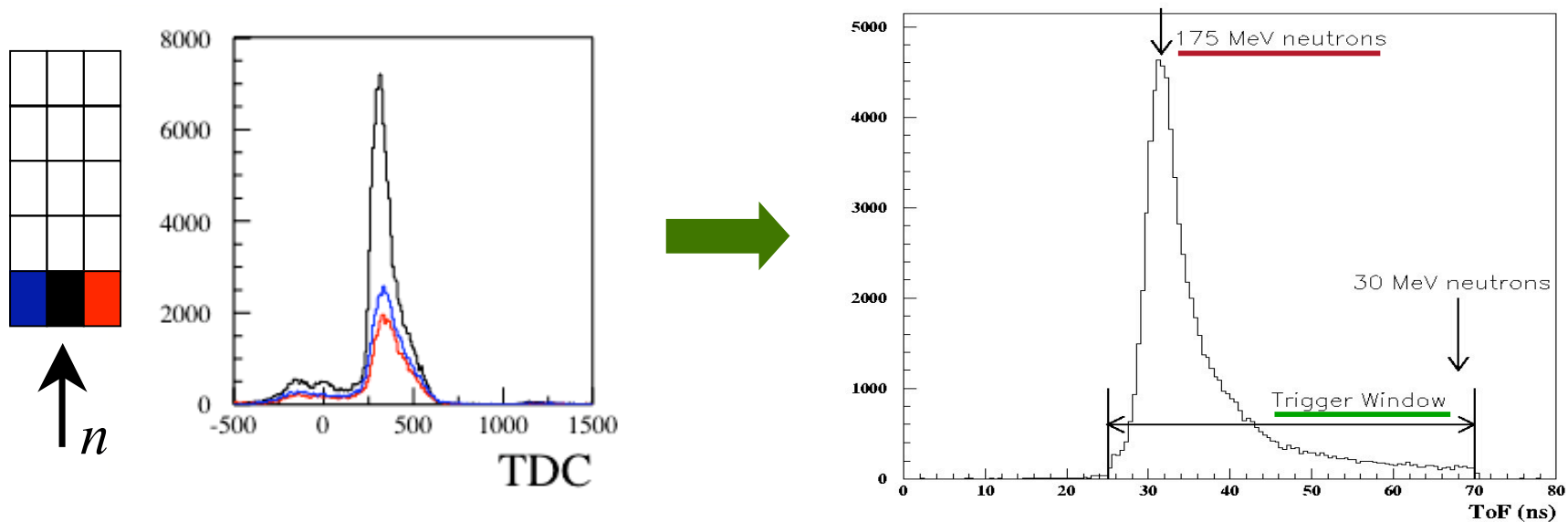
MeV eq. el. en.



Thr. [mV]	15 → 75
Thr. [MeV]	5.3 → 22.8

# Energy spectrum from TOF

- *Energy spectrum can be reconstructed from TOF*



- *Rephasing is needed, since the trigger is phase locked with the RF (45 ns period)*
- *From TOF  $\Rightarrow$   $\beta$  spectrum of the neutrons*
- *Assuming the neutron mass  $\Rightarrow$  kinetic energy spectrum*

# *Background subtraction: the beam halo evaluation*

---

- *Data reconstructed clusters with a single fired cell show a ratio **lateral/central** fired cells **higher** than in MC*
- *Lateral cells show also a flatter time distribution compared with MC*



*Background due to low energy neutrons forming a halo around the beam core*

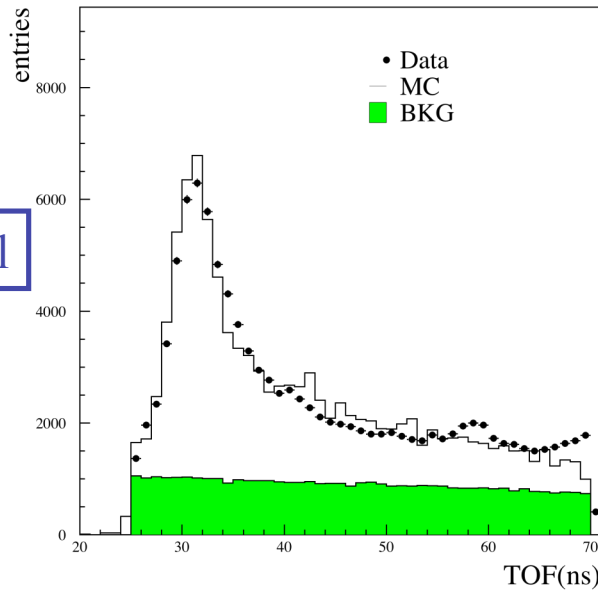
- ***TOF distributions*** of data have been fit with:
  - *a linear parametrization for the background;*
  - *the MC shape for the signal*for each single calorimeter plane *and* for each trigger threshold



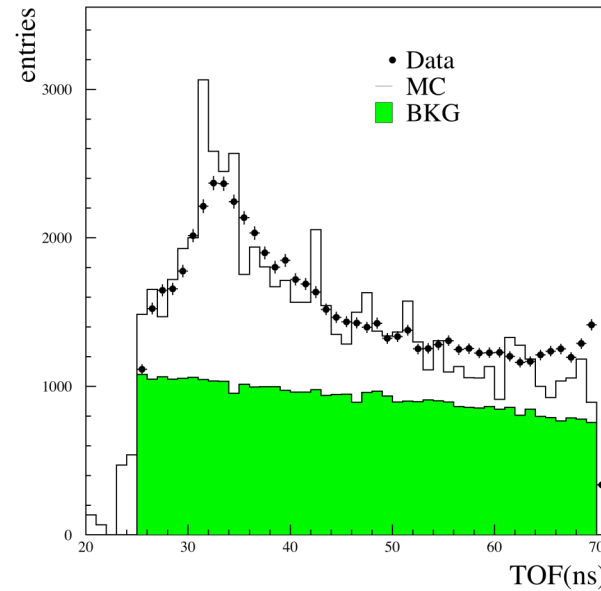
***The halo fraction has been measured for each trigger threshold***

# Beam halo @ 174 MeV

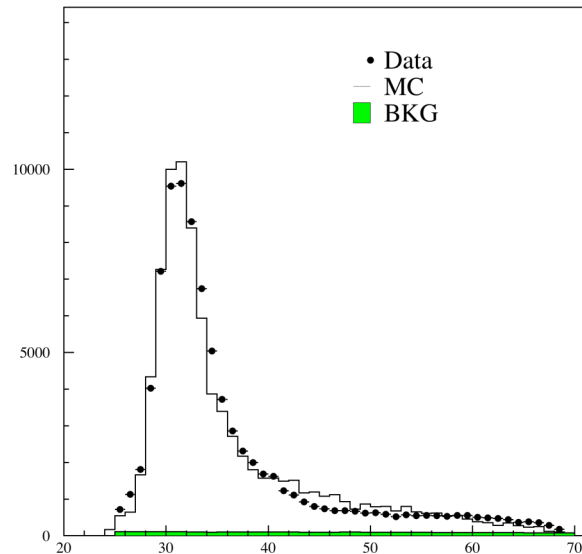
Central cell



Outer cell



Cluster with more than 1 cell



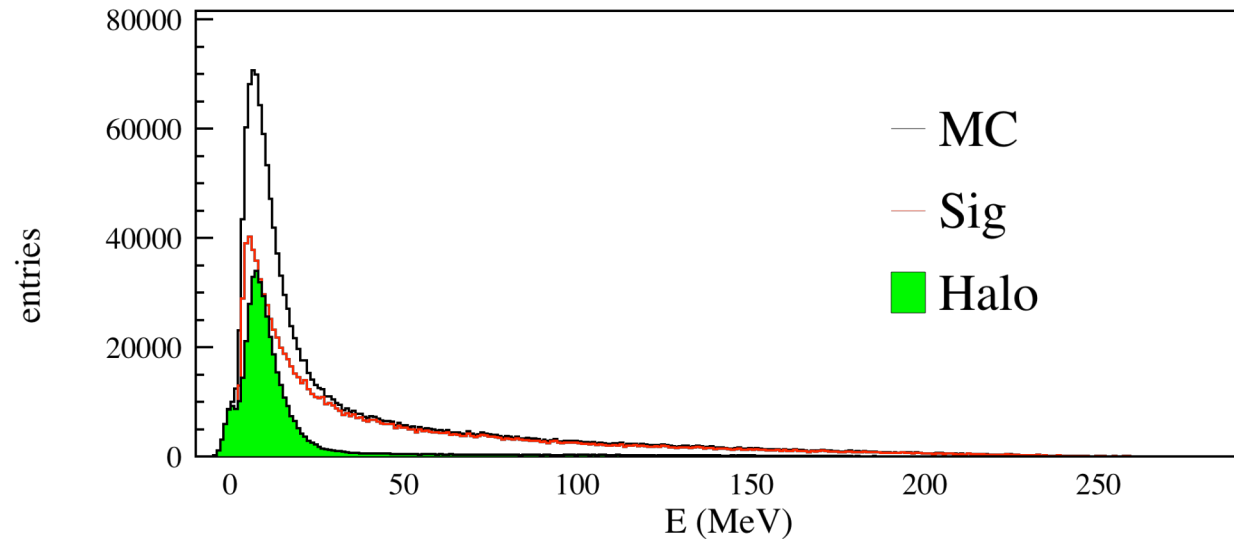
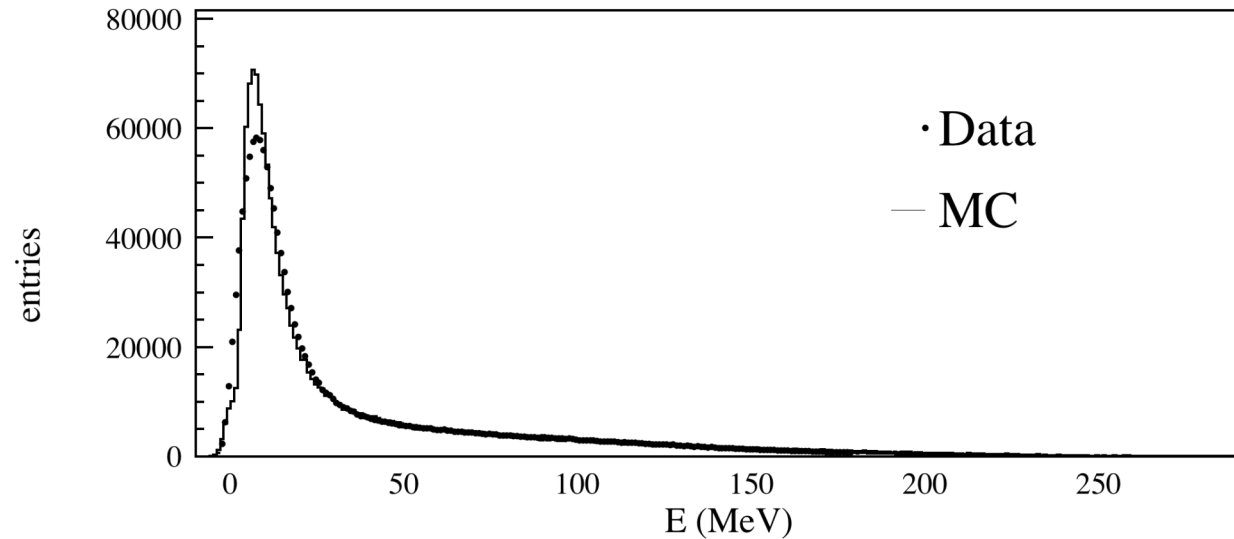
Good agreement taking into account halo contribution.  
Halo amount obtained fitting TOF from outer cells.

We estimate a contribution of 30% of the total number of events for halo neutrons.



# Cross-check with Q response

The halo contribution can be checked looking at other variables.



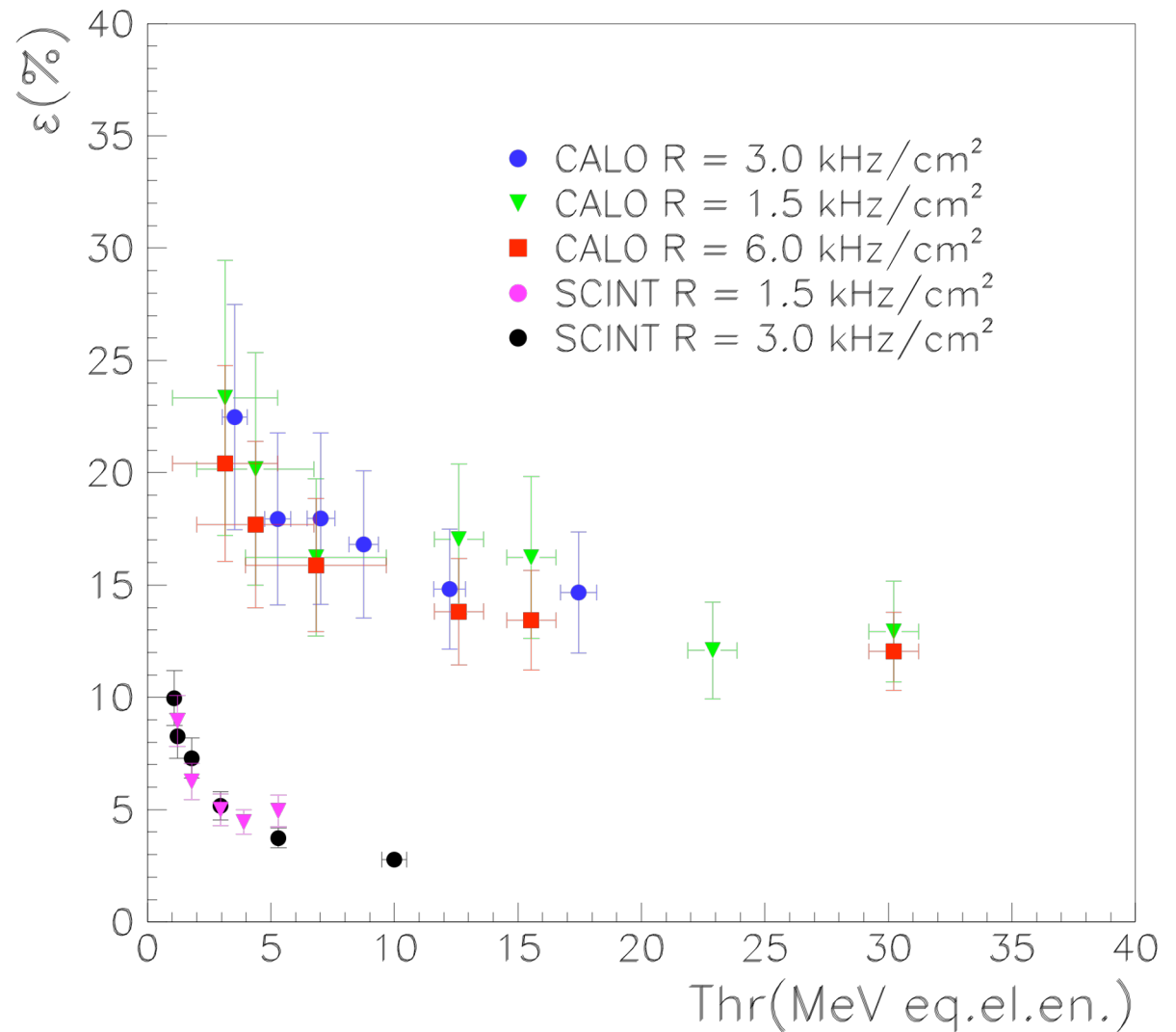
# Beam halo @ 21,46 MeV

---

- While completing a similar TOF study, at low energy we still rely on halo measurement carried out by TSL beam experts
  - They performed a TFBC scan of the area near the collimator
    - ⇒ integrated flux over the ICM area ~ 5% of the “core” flux  
(with large uncertainty)
    - ⇒ halo shape also measured
- Confirmed by our background counters
- Our calorimeter is larger than the projection of ICM area
- By integrating over the calorimeter we estimate  $F_h = (20 \pm 10)\%$
- Only 10% on the reference scintillator due to the smaller area

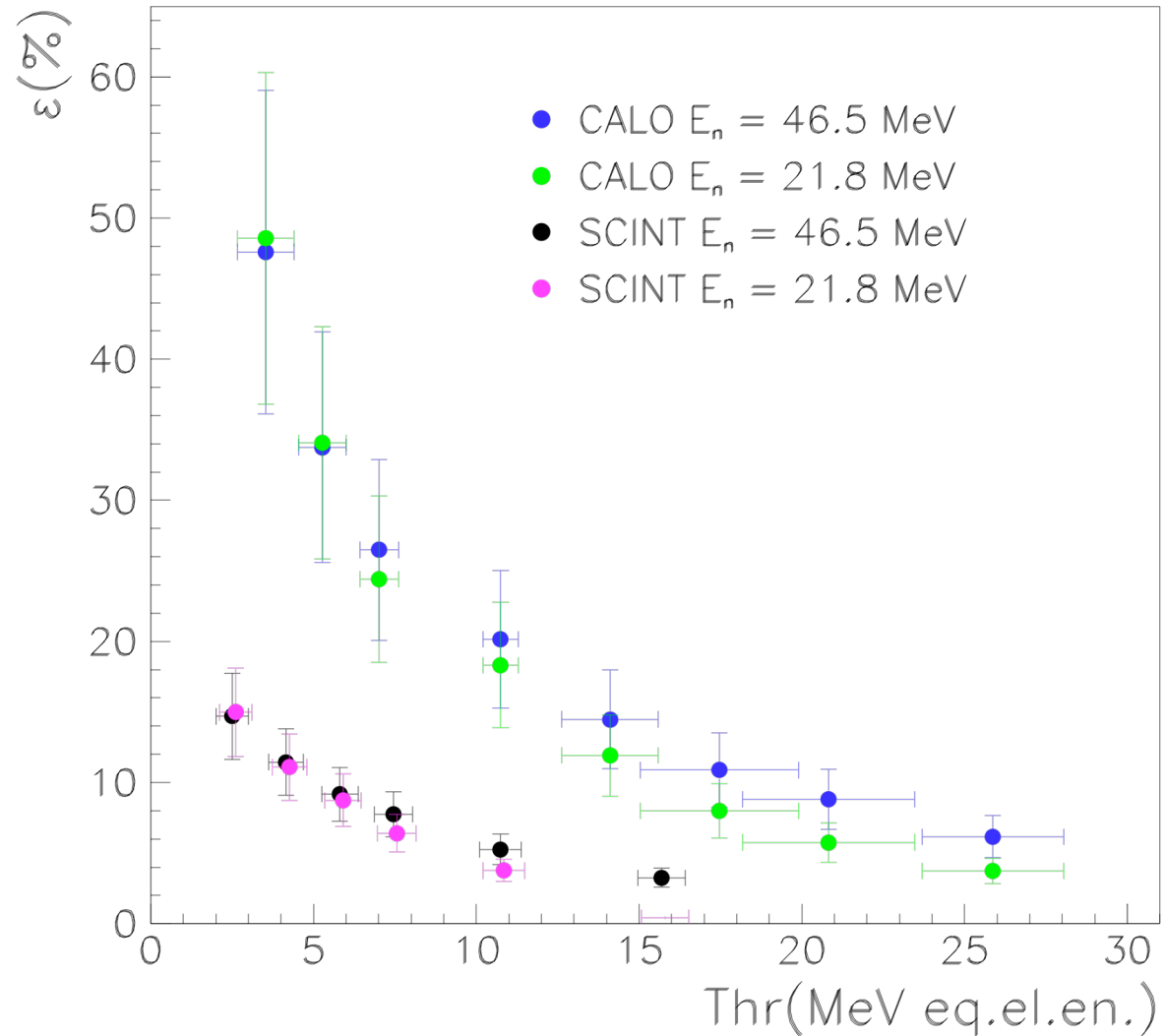
# Calo efficiency: results @ 174 MeV

- *Very high efficiency at low threshold*
- *Agreement between high and low energy measurements*



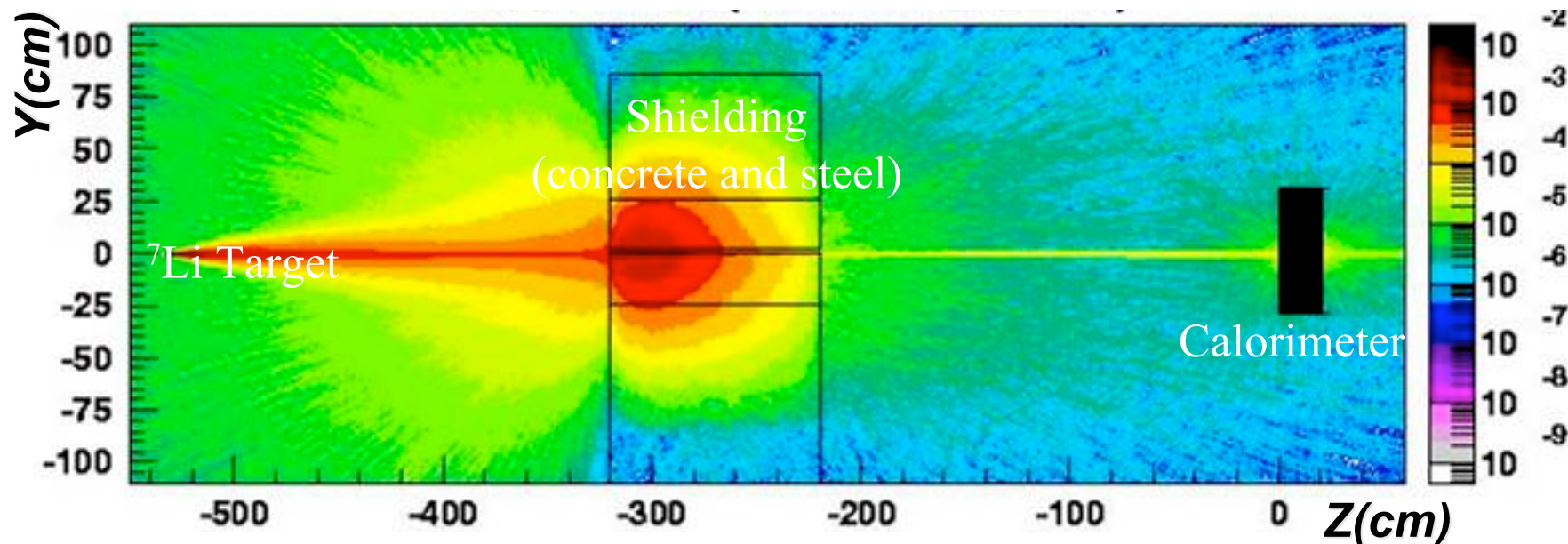
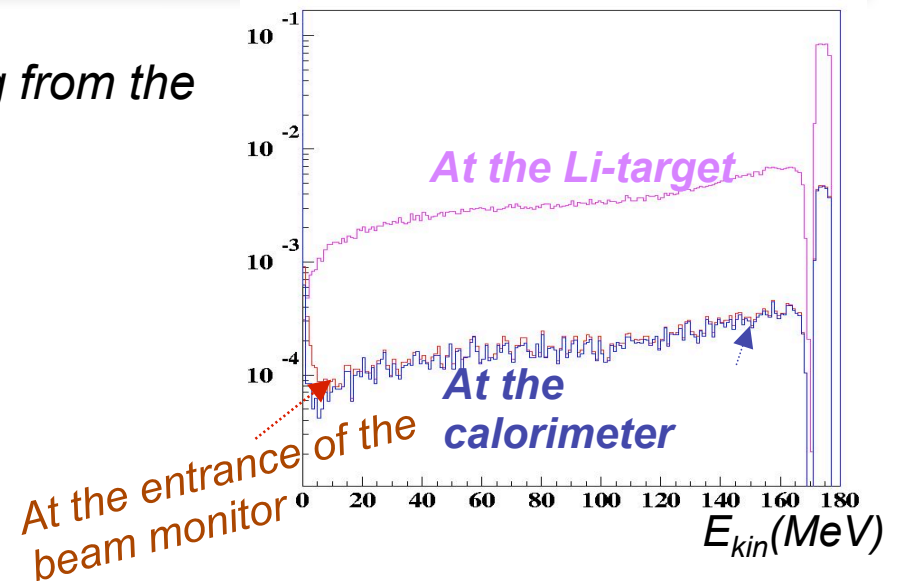
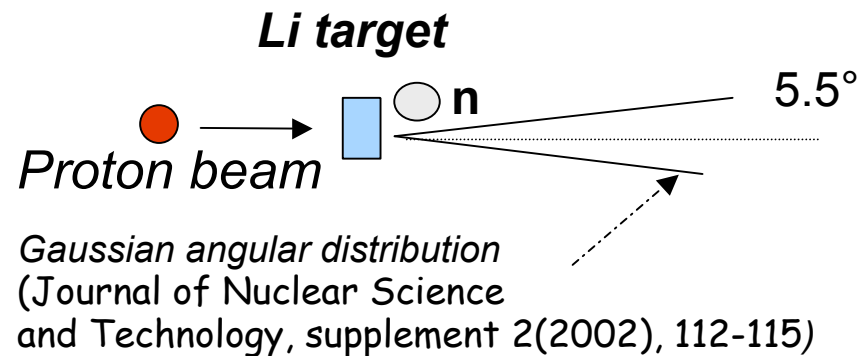
# Calo efficiency: results @ 21,46 MeV

- *Very high efficiency at low threshold*
- *Agreement between high and low energy measurements*



# The simulation of the beam line

- The beam line has been simulated starting from the neutrons out of the Lithium target



# The FLUKA simulation - part (I)

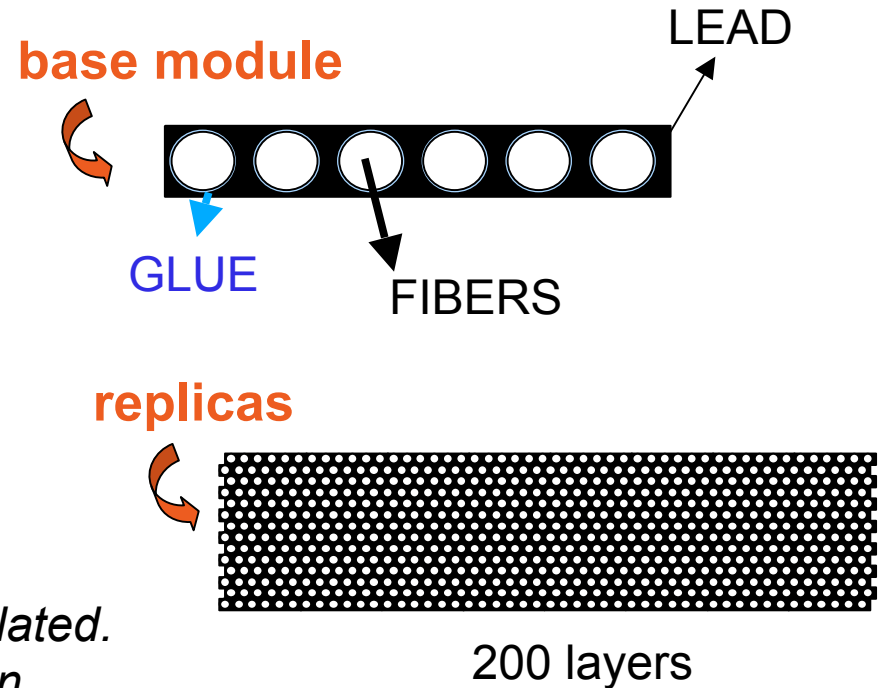
## The Pb-SciFi structure

➤ Using the FLUKA tool LATTICE the fiber structure of the whole calorimeter module has been designed.

➤ In the base module the calorimeter is simulated in detail, both under the **geometrical** point of view and with respect to the used **materials**

- All the compounds have been carefully simulated.
- for the **fibers**, an average density between cladding and core has been used :  $\rho = 1.044 \text{ g/cm}^3$
  - **glue**: 72% **epoxy resin**  $\text{C}_2\text{H}_4\text{O}$ ,  $\rho=1.14 \text{ g/cm}^3$ ,  
+ 28% **hardener**,  $\rho=0.95 \text{ g/cm}^3$

*hardener composition*



Polyoxypropyldiamine	$\text{C}_7\text{H}_{20}\text{NO}_3$	90%
Triethanolamine	$\text{C}_6\text{H}_{15}\text{NO}_3$	7%
Aminoethylpiperazine	$\text{C}_6\text{H}_{20}\text{N}_3$	1.5%
Diethylenediamine	$\text{C}_4\text{H}_{10}\text{N}_2$	1.5%



# Neutron interactions in the calorimeter

Simulated neutron beam:  $E_{kin} = 180 \text{ MeV}$

Each primary neutron has a high probability to have elastic/inelastic scattering in Pb

In average, secondaries generated in **inelastic interactions** are **5.4** per primary neutron, counting only neutrons above 19.6 MeV.

Typical reactions on lead:



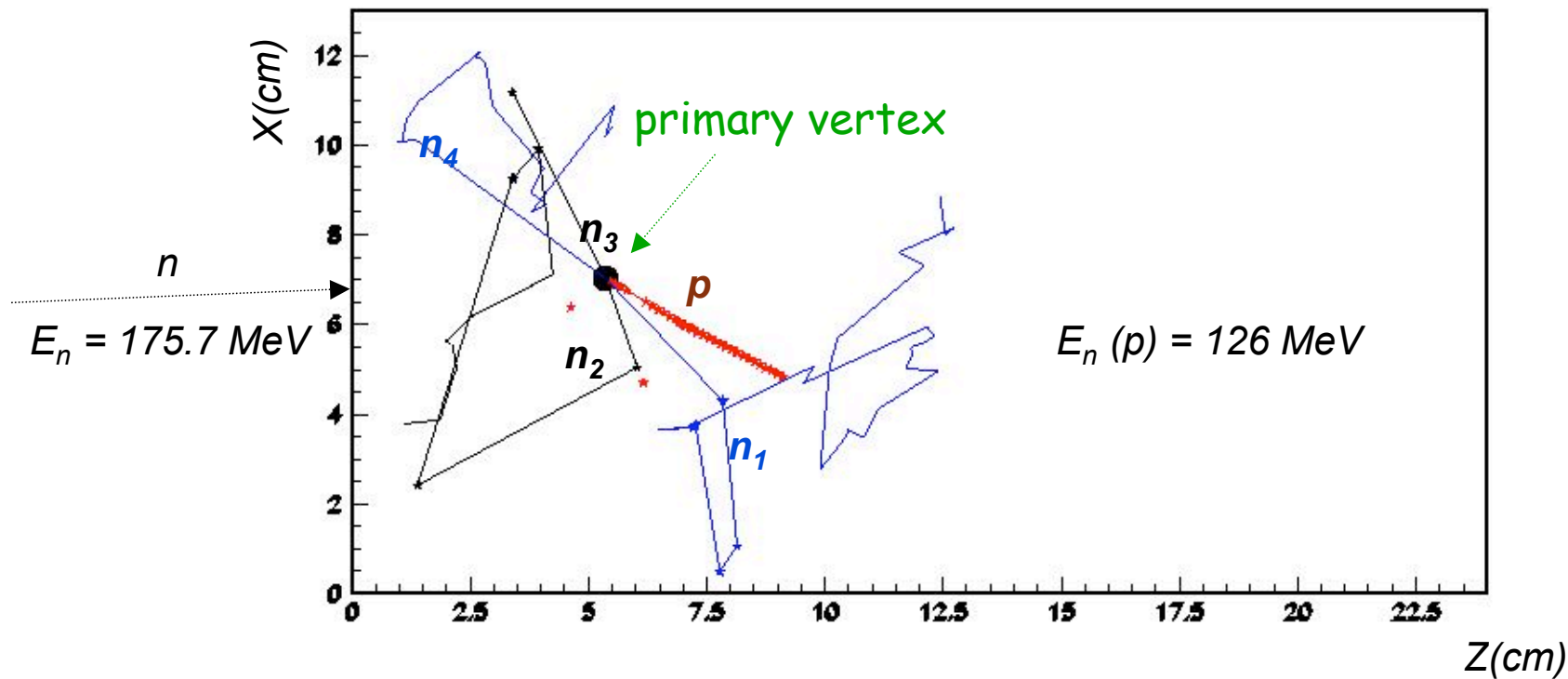
In addition, secondaries created in interactions of low energy neutrons (below 19.6 MeV) are - in average - **97.7** particles per primary neutron.

target	$P_{el}(\%)$	$P_{inel}(\%)$
<i>Pb</i>	32.6	31.4
<i>fibers</i>	10.4	7.0
<i>glue</i>	2.3	2.2

<i>neutrons</i> <i>above 19.MeV</i>	62.2%
<i>photons</i>	26.9%
<i>protons</i>	6.8%
<i>He-4</i>	3.2%
<i>deuteron</i>	0.4%
<i>triton</i>	0.2%
<i>He-3</i>	0.2%

<i>neutrons</i>	94.2%
<i>protons</i>	4.7%
<i>photons</i>	1.1%

# A typical inelastic process



The enhancement of the efficiency appears to be due to the **huge inelastic production of neutrons on the lead planes**. These secondary neutrons:

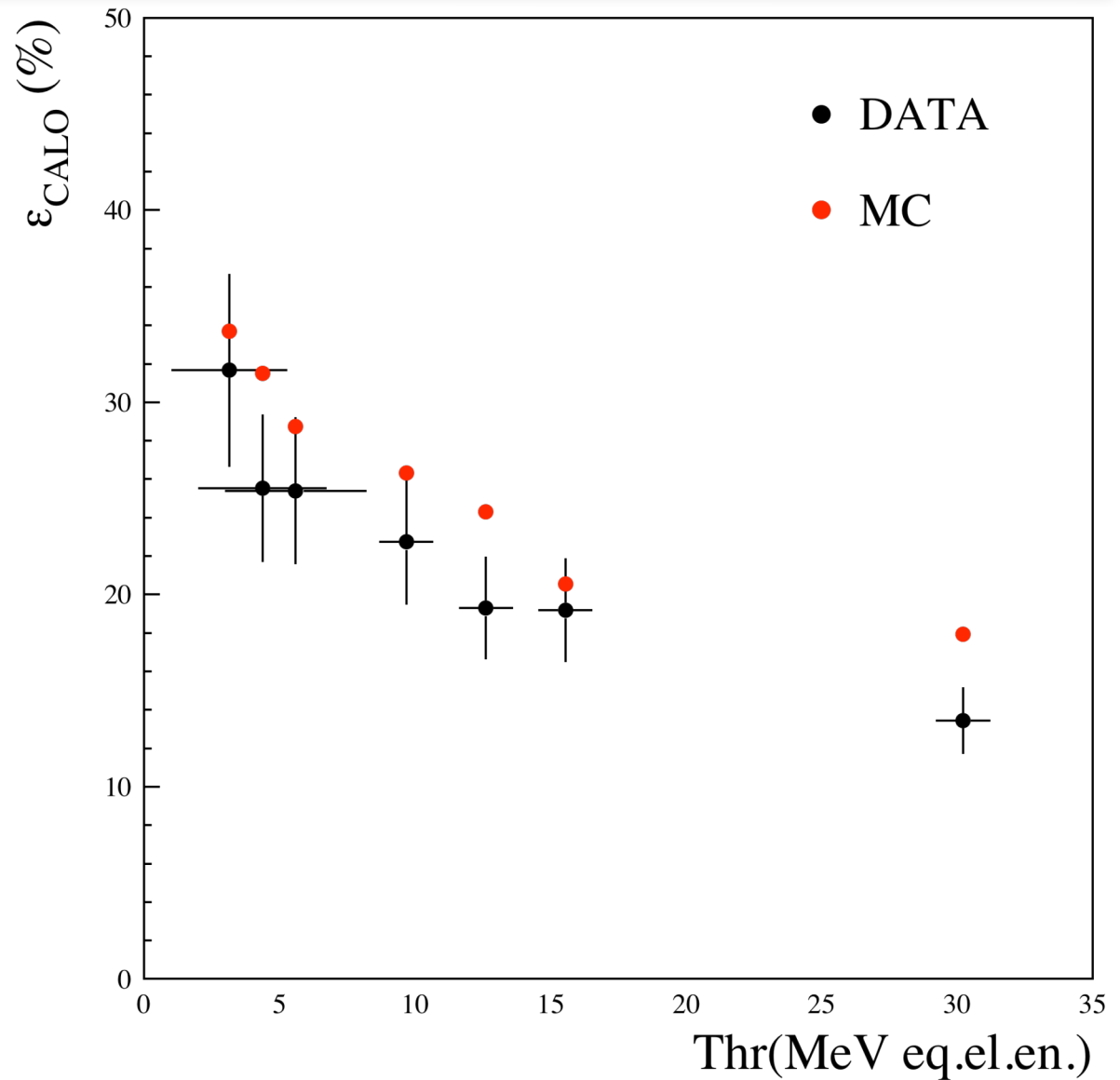
- are produced isotropically;
- are produced with a non negligible fraction of e.m. energy and of protons, which can be detected in the nearby fibers;
- have a lower energy and then a larger probability to do new interactions in the calorimeter with neutron/proton/ $\gamma$  production.

# Preliminary Data/MC comparison

Run @ 174 MeV

Efficiency comparison  
between DATA and  
simulation as a function of  
the applied trigger  
threshold.

Halo contribution taken  
into account.



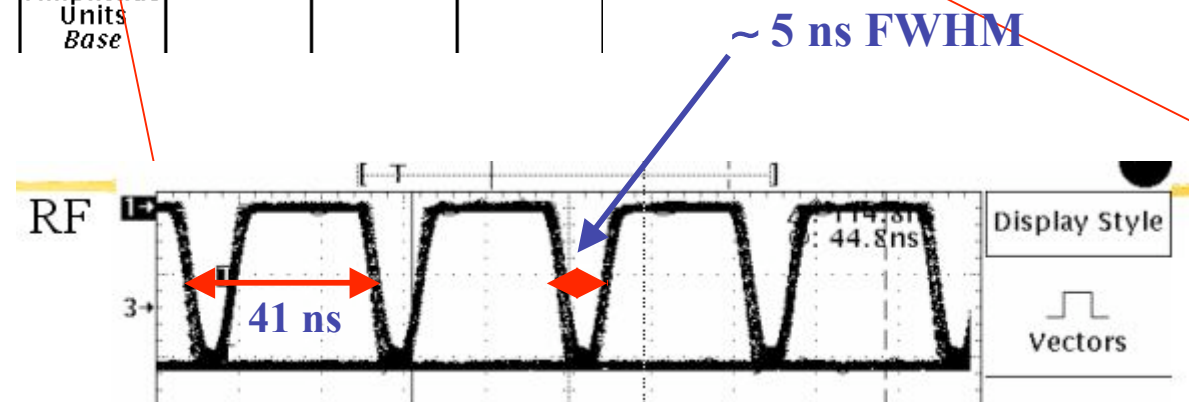
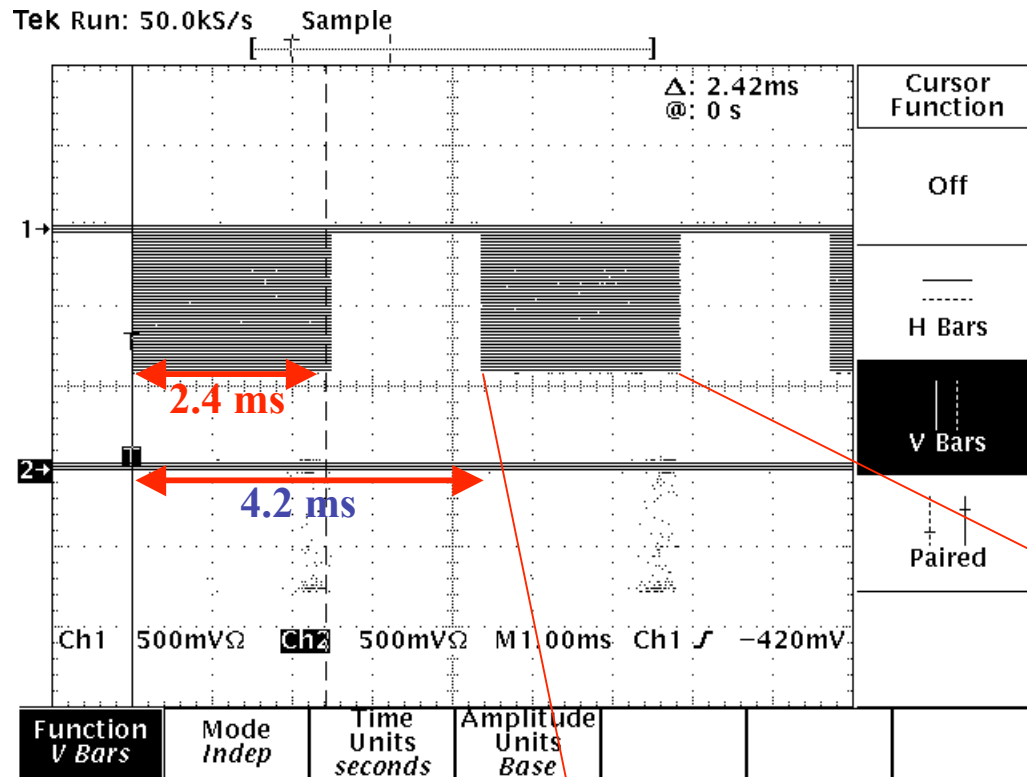
# Conclusions

---

- *The first measurement of the detection efficiency for neutrons of 20 - 180 MeV of a high sampling Pb-sci.fi. calorimeter has been performed at TSL*
- *The cross-check measurement of the n efficiency of a NE110 scintillator agrees with published results in the same energy range.*
- *The calorimeter efficiency, integrated over the whole neutron energy spectrum, ranges between 32-50 % at the lowest trigger threshold, and results between 3-4 times larger than what expected for the equivalent scintillator thickness.*
- *Full simulation with FLUKA is in progress, first results are encouraging.*
- *Further test foreseen for fall 2008 at TSL with:*
  - *a new BPM counter with X-Y readout, high granularity*
  - *the high granularity prototype of KLOE calorimeter*
  - *a small calorimeter with different sampling fraction (more lead).*

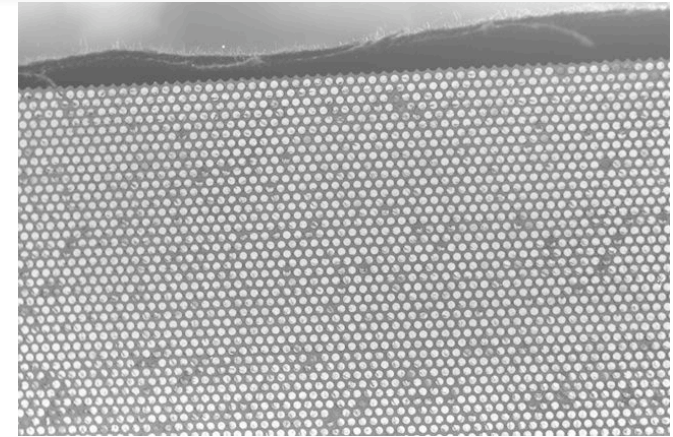
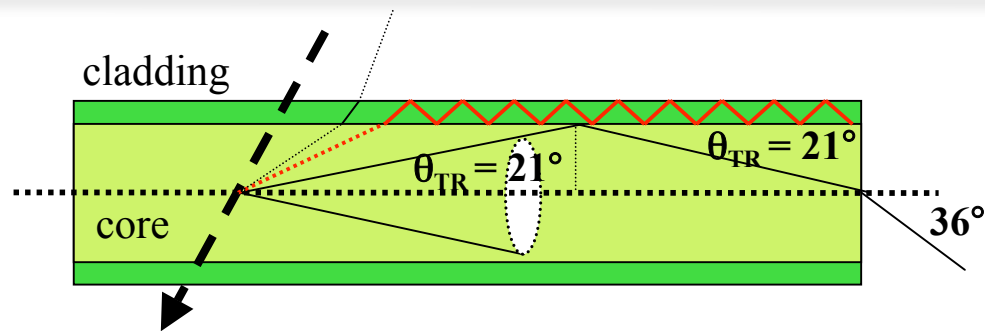
# Spares

# Beam time structure



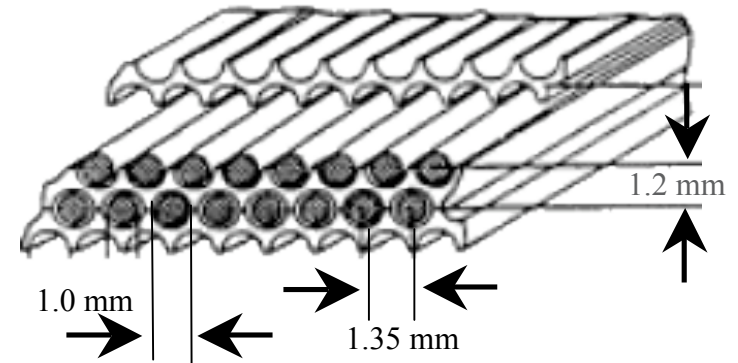


# Calorimeter details



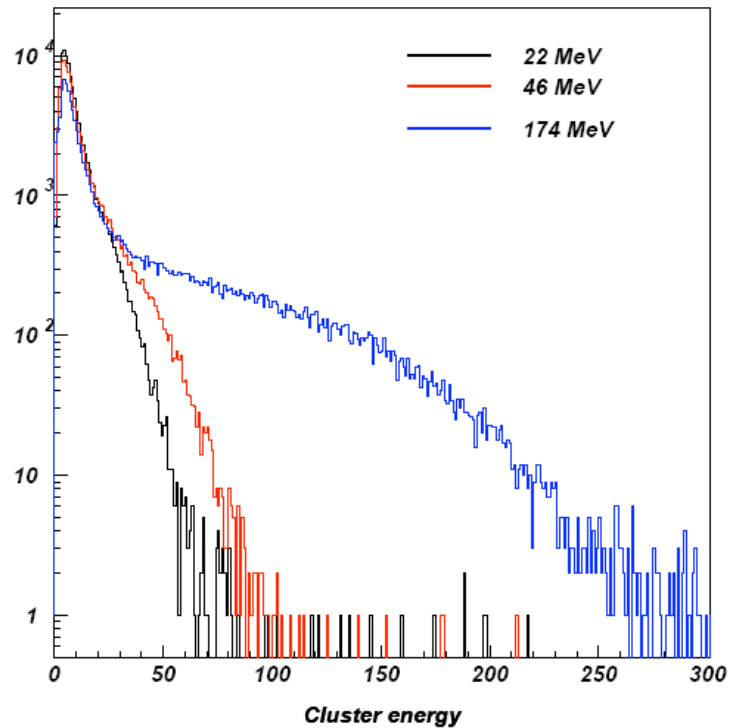
- 1 mm diameter scintillating fiber (Kuraray SCSF-81, Pol.Hi.Tech 0046), emitting in the blue-green region,  $\lambda_{\text{Peak}} < 460\text{nm}$ .
- 0.5 mm lead grooved layers (95% Pb and 5% Bi).
- Glue: Bicorn BC-600ML, 72% epoxy resin, 28% hardener.
- Core: polystyrene,  $\rho=1.050\text{ g/cm}^3$ ,  $n=1.6$
- Cladding: PMMA,  $n=1.49$
- Only  $\sim 3\%$  of produced photons are trapped in the fiber.

But: small transit time spread due to uni-modal propagation at  $21^\circ$ , small attenuation ( $\lambda=4\text{-}5\text{m}$ ), optical contact with glue ( $n_{\text{GLUE}} \sim n_{\text{CORE}}$ ) remove cladding light

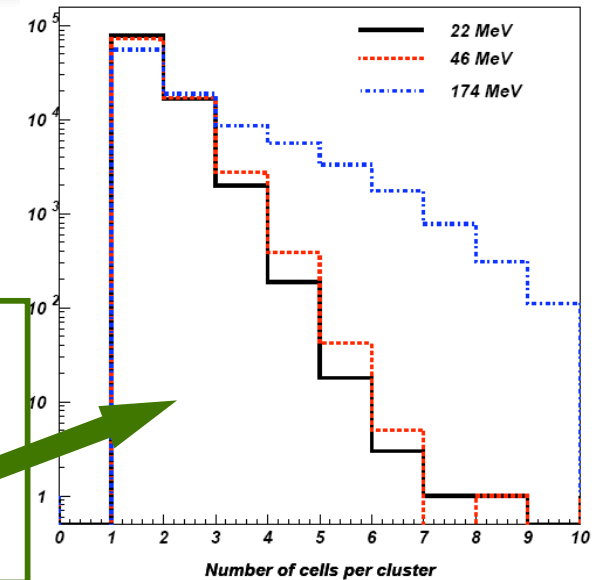


# Events anatomy

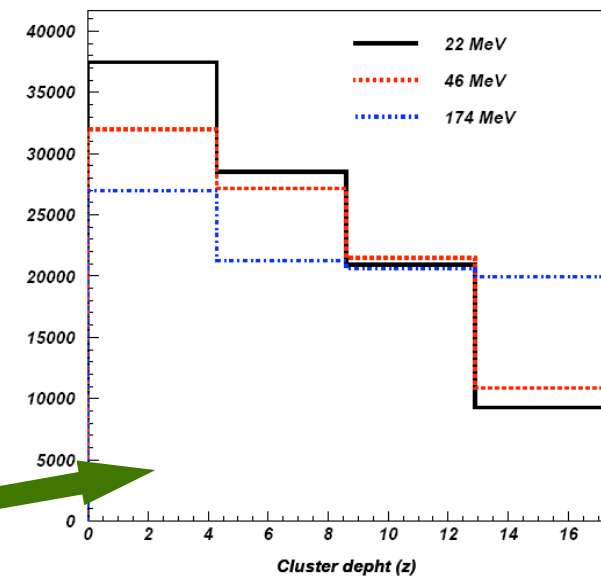
Energy deposited by neutrons for the three beam energies



Number of cells per neutron cluster increases with beam energy



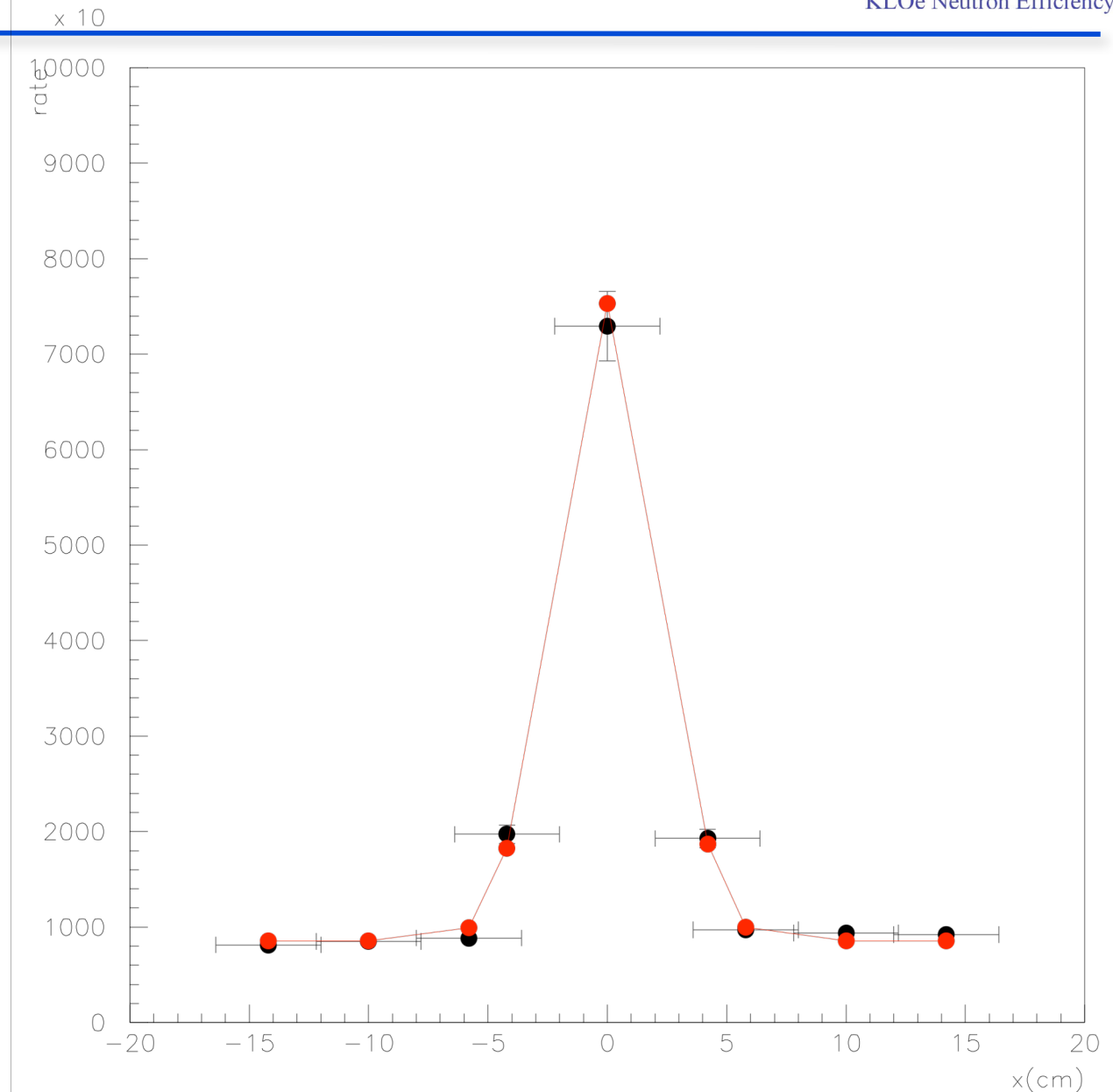
Position of neutron clusters in the calorimeter along the forward direction



# Halo evidence

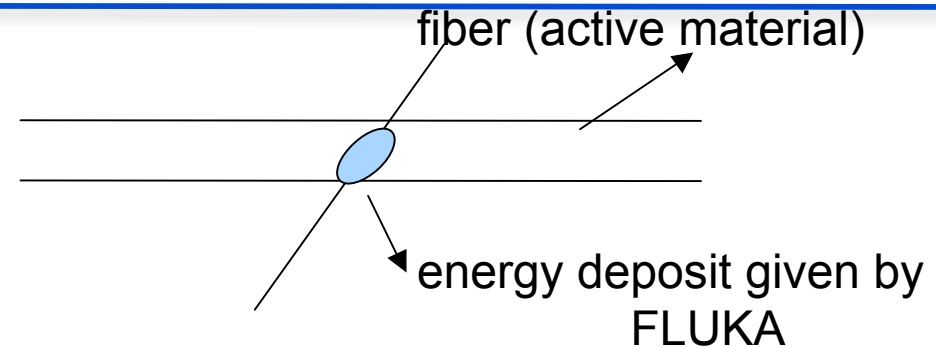
Moving calorimeter on “x” direction respect to the zero, we can have an evidence of the halo excluding the signal due to the beam.

The halo contributes for the flat component around the central beam core.



# Simulation of the energy read-out

The light is propagated by hand at the end of the fiber using the parametrization:



$$E_{a,b}^{(fib)} = E_{(dep)} \cdot [0.35 e^{-x(a,b)/50} + (1-0.35) e^{-x(a,b)/430}] \quad \text{Kuraray}$$

**Attenuation**

$$E_{a,b}^{(fib)} = E_{(dep)} \cdot [0.35 e^{-x(a,b)/50} + (1-0.35) e^{-x(a,b)/330}] \quad \text{Politech}$$

$$t_{a,b}^{(fib)} = t_{(dep)} + X_{(a,b)}/17.09$$

The number of photoelectrons generated by the light collected by each fiber is evaluated.

$$n_{a,b}^{(pe-fib)} = E^{(fib)}(MeV)_{(a,b)} \cdot 25$$

$n_{a,b}^{pe\_fib}$  generated according to a Poisson distribution

$$t_{(a,b)}^{(p.e.)} = t_{(a,b)}^{(fib)} + t_{scin} + 1ns \text{ (smearing)}$$

$$n_{a,b}^{(pe-cell)} = \sum_{t(pe) < 300ns} n_{a,b}^{pe\_fib}$$

the constant fraction distribution is simulated (15% fr., 10 ns t.w.) to obtain the time

## The readout simulation

---

Fluka gives *energy deposits* in the fiber.

The light is propagated 'by hand' at the end of the fiber taking into account the attenuation.

The energy read-out has been simulated by including:

- ❖ the generation of photoelectrons
- ❖ the constant fraction distribution
- ❖ the discriminator threshold.
- No trigger simulation is included at the moment.

## The simulation of the Birks effect

The energy deposits are computed in Fluka **taking into account the Birks effect**, that is the saturation of the light output of a scintillating material when the energy release is high, due to the quenching interactions between the excited molecules along the path of incident particles:

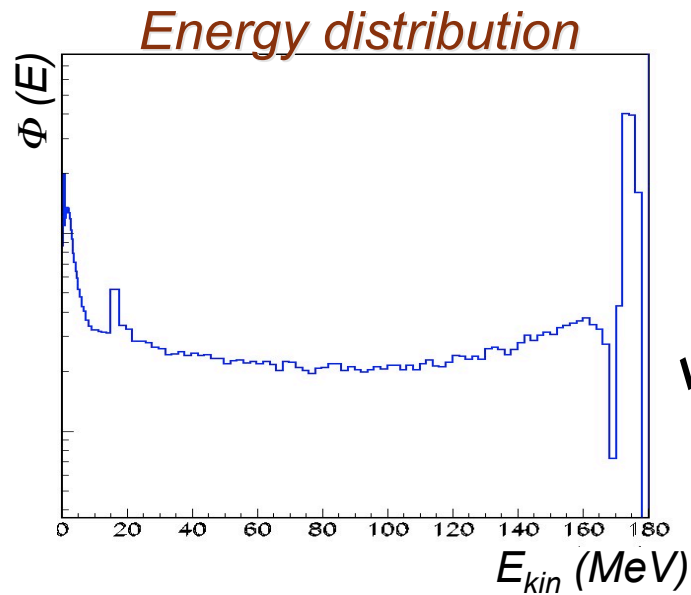
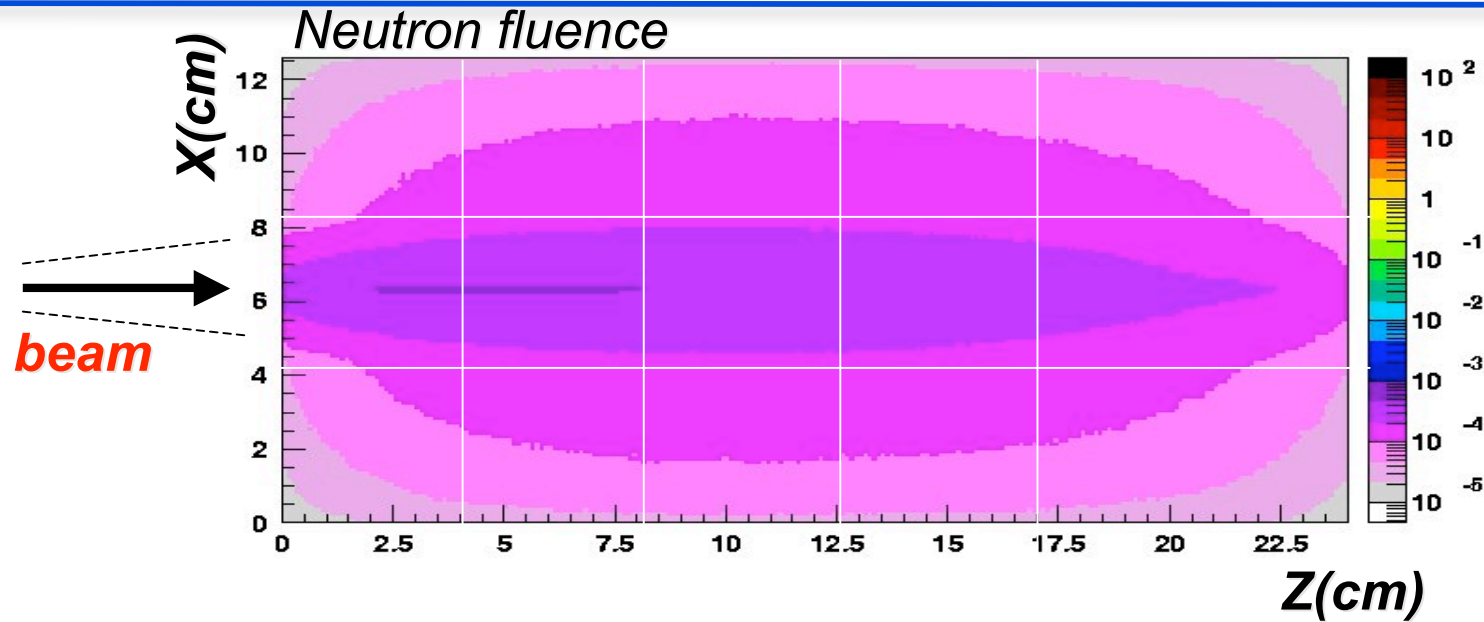
$$dL/dx = k \, dE/dx / [ 1 + c_1 \, dE/dx + c_2 \, (dE/dx)^2 ]$$

In literature and in GEANT:

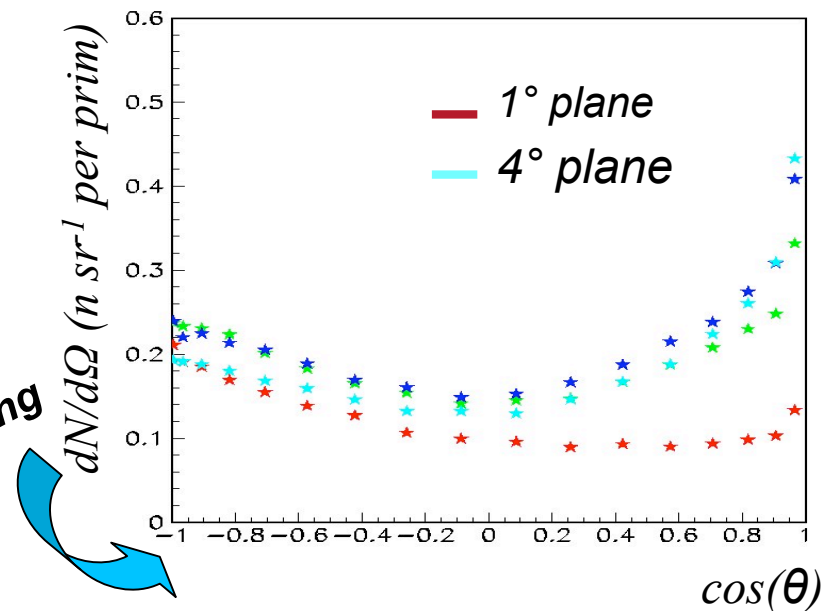
$$c_1 = 0.013$$

$$c_2 = 9.6 \times 10^{-6}$$

# Neutron yield inside the calorimeter



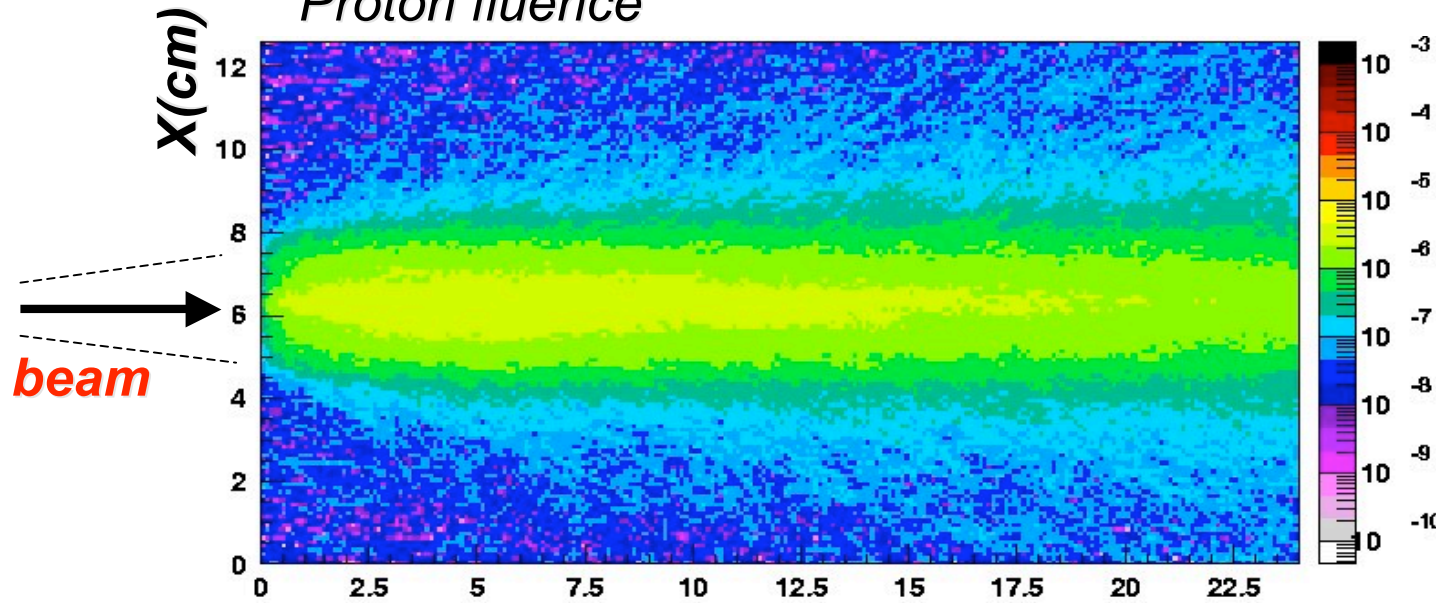
Isotropic angular distributions from inelastic scattering





# Proton yield inside the calorimeter

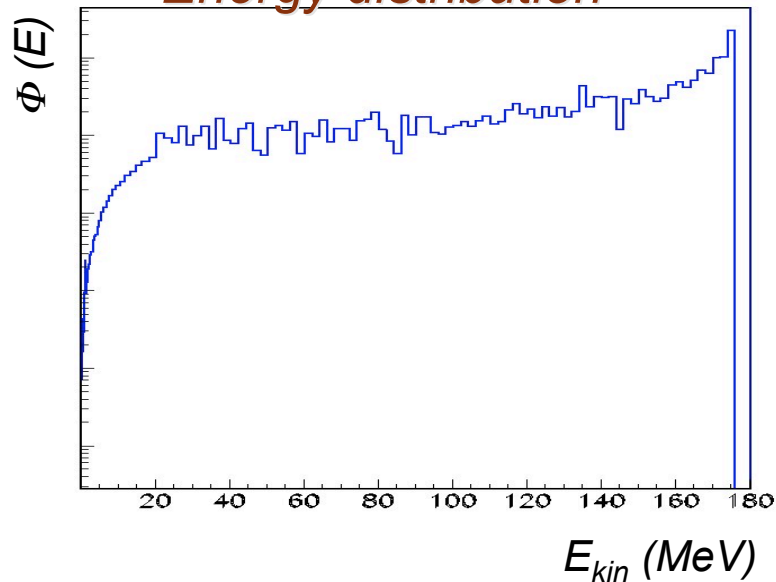
Proton fluence



Protons are mainly concentrated along the direction of the primary beam

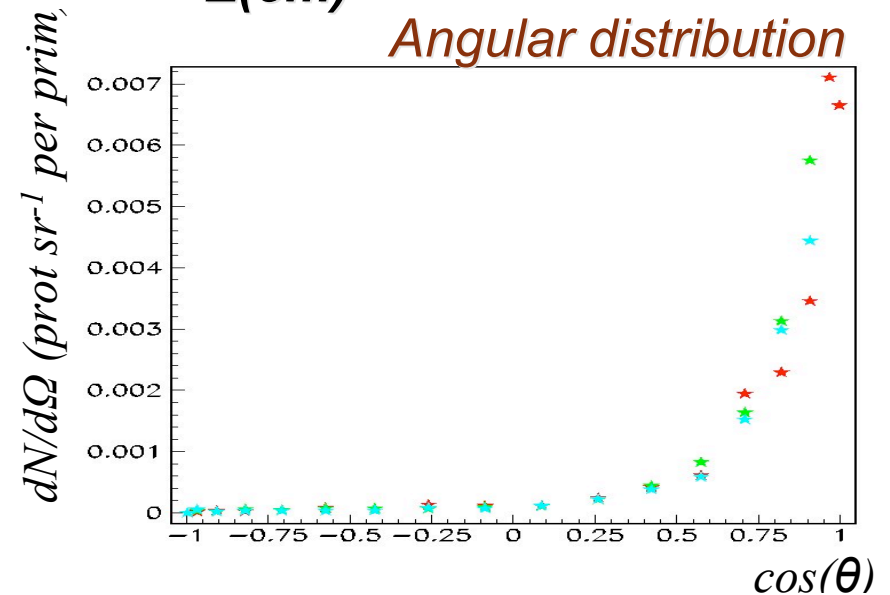


Energy distribution



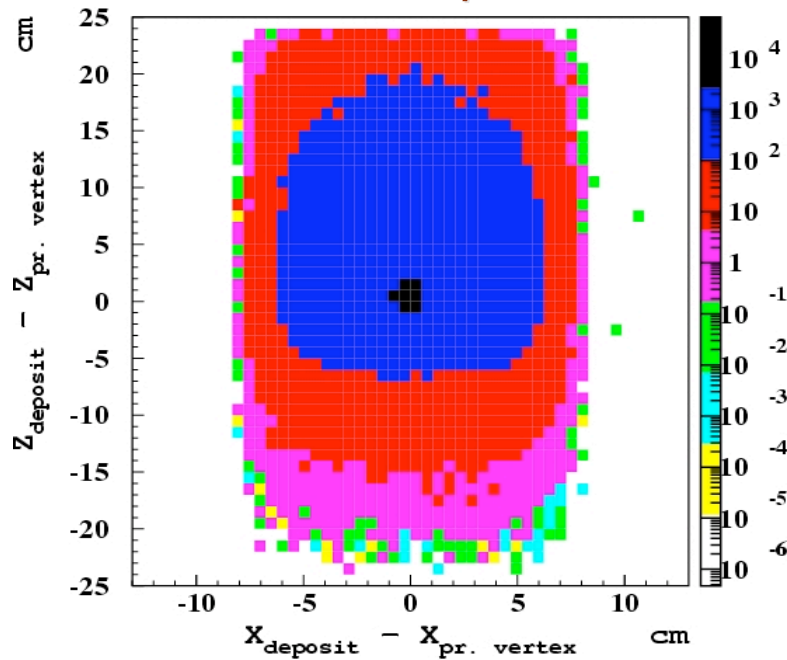
$Z(\text{cm})$

Angular distribution

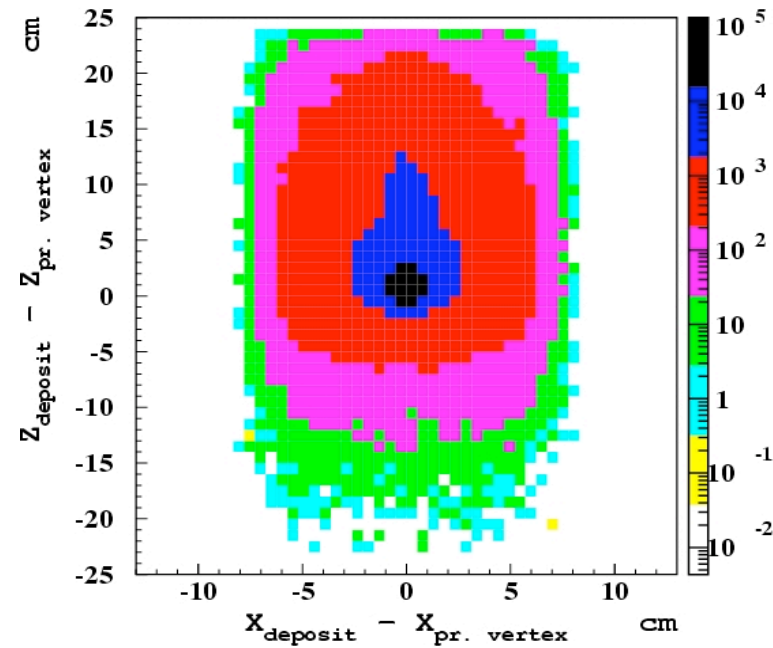


# *A key point: the high sampling frequency*

*neutron lateral profile*



*proton lateral profile*



*The energy deposits of the ionizing particles (protons and excited nuclei) are distributed mainly in the nearby fibers:*

 *the high sampling frequency is crucial in optimizing the calorimeter*